Mesoporous Materials

DOI: 10.1002/anie.201107460

Conversion of Sb_2Te_3 Hexagonal Nanoplates into Three-Dimensional Porous Single-Crystal-Like Network-Structured Te Plates Using Oxygen and Tartaric Acid**

*Hua Zhang, Huan Wang, You Xu, Sifei Zhuo, Yifu Yu, and Bin Zhang**

Novel applications of nanostructures in catalysis, electronics, photonics, and bionanotechnology[1] are driving the exploration of synthetic approaches to control and manipulate their chemical composition, structure, and morphology.[2–5] As well as the design of synthetic strategies to produce a new class of nanoscale materials, recent developments have enabled the chemical transformation of one crystalline material into another desired target material.[2] Three of the most important methods for chemical transformation are the ion-exchange reaction,[3] the Kikendall effect,[4] and stabilizer-depleted binary semiconductor nanocrystals.[5] The first two methods have been shown to produce nanomaterials with a diverse structure and a controlled composition, but are not suitable to transform binary materials into unary semiconductors. Interestingly, the third method has been successfully adopted by Kotov and Tang et al. to convert CdE (E = Se, Te) into unary E solid nanowires and angled Te nanocrystals.[5] Among the various materials, porous nanostructures have received increasing attention owing to their improved chemical and physical performance over solid materials, as well as their intriguing applications in a variety of fields.[6] In comparison with their polycrystalline counterparts, single-crystal-like materials have been found to reduce the number of defects, and have enhanced electron-transfer and catalytic properties.[7] However, the development of a facile technique to transform binary materials into three-dimensional (3D) porous unary semiconductors, especially with single-crystal-like structures, remains a great challenge.

Herein we report a facile approach to transform the as-prepared Sb_2Te_3 nanoplates into 3D porous Te plates through the dissolution of Sb^{3+} ions, the oxidation of Te^{2-} ions to Te^0, and a subsequent Ostwald ripening process induced by oxygen and tartaric acid (TA). We have demonstrated that this method can be adopted to convert Sb_2Te_3 nanoplates into porous heterogeneous In/Te networks through the reduction of $InCl_3$ during the chemical transformation of Sb_2Te_3. Furthermore, the as-prepared porous Te plates can be used as the template for the highly efficient synthesis of 3D porous network-structured noble-metal nanoplates with promising applications.

Firstly, the Sb_2Te_3 hexagonal nanoplates were synthesized by using the reported solution–chemical method.[8] Figure 1 a shows a scanning electron microscopy (SEM) image of hexagonal nanoplates with a thickness of 50–200 nm. The typical powder X-ray diffraction (XRD) pattern displayed in Figure 1 f identifies these hexagonal plates as the rhombohe-

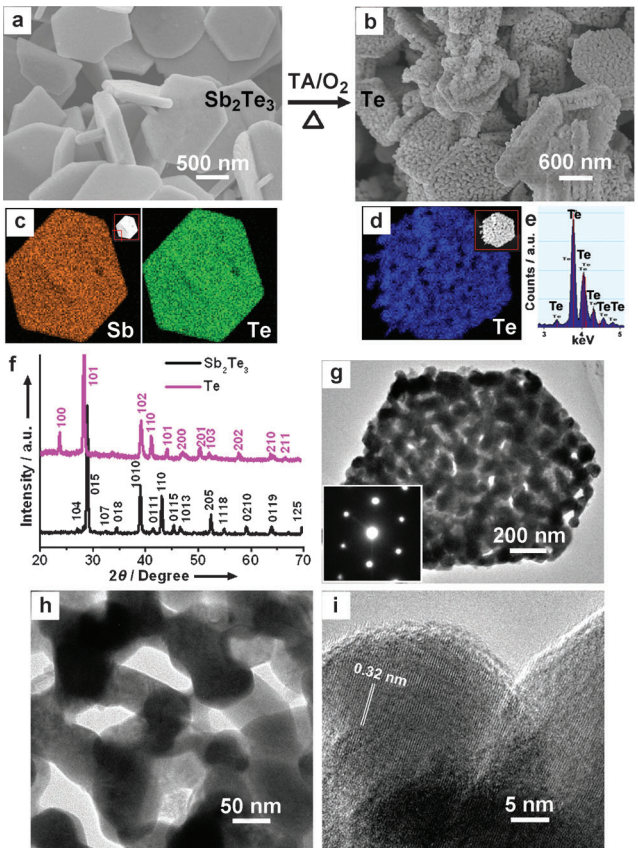

Figure 1. SEM images of a) the starting Sb_2Te_3 nanoplates and b) the 3D porous network-structured Te plates, EELS mapping elemental images of c) the starting Sb_2Te_3 nanoplates and d) the 3D porous Te plates, e) EDX image of the 3D porous Te plates, and f) XRD patterns. g,h) TEM images and i) HRTEM image of the as-prepared 3D porous network-structured Te nanoplates obtained through the chemical transformation of the Sb_2Te_3 plates. The inset in Figure 1 g is the associated SAED pattern of one porous network-structured Te plate.

[*] H. Zhang,[+] H. Wang,[+] Y. Xu, S. Zhuo, Y. Yu, Prof. Dr. B. Zhang
Department of Chemistry, School of Science
Tianjin University, Tianjin 300072 (P.R. China)
E-mail: bzhang@tju.edu.cn

[+] These authors contributed equally to this work.

[**] This work was financially supported by the National Natural Science Foundation of China (20901057 and 11074185), the National Basic Research Program of China (2009CB939901), the Tianjin Natural Science Foundation (10JCYBJC01800), the State Key laboratory of Crystal Material at Shandong University (KF0910) and the Innovation Foundation of Tianjin University.

Supporting information for this article is available on the WWW under http://dx.doi.org/10.1002/anie.201107460.

dral phase of Sb_2Te_3 (JCPDS 15-0874), thus suggesting that the Sb_2Te_3 nanoplates can be successfully fabricated. For a typical transformation of the Sb_2Te_3 nanoplates, the aqueous solution containing the as-prepared Sb_2Te_3 hexagonal nanoplates (Figure 1a) and TA was hydrothermally treated at 180 °C for 6 hours in the presence of a trace amount of oxygen. Figure 1b and Figure S1 in the Supporting Information display scanning electron microscopy (SEM) images of the as-converted products, and indicate the 3D porous morphology of the products. The chemical transformations are further characterized using electron energy loss spectroscopy (EELS) elemental mapping. As shown in Figure 1c, Sb and Te elements are uniformly distributed in a solid hexagonal plate. However, after the Sb_2Te_3 nanoplate was hydrothermally treated in the presence of TA and oxygen, only the Te element, with porous distribution, is seen in the EELS mapping of the porous plate (Figure 1d). This implies that the Sb^{3+} ions of the Sb_2Te_3 nanoplates can be stripped and dissolved into aqueous solution. The energy-dispersion X-ray fluorescence (EDX) spectrum (Figure 1e and Figure S2 in the Supporting Information) also confirms that the as-transformed porous networks are composed of pure tellurium. The crystal structure and phase composition of the porous network-structured products obtained are characterized using X-ray powder diffraction (XRD). Figure 1f shows the XRD pattern of the porous Te samples, in which all the diffraction peaks can be indexed to the trigonal phase of Te (JCPDS 36-1452). This indicates that the Sb_2Te_3 solid plates can be completely transformed into porous Te nanoplates with high purity. These results suggest that the complete conversion of Sb_2Te_3 into highly pure 3D porous Te nanoplates can be achieved in the current approach.

The morphology and structure of the porous network-structured Te products were further examined by transmission electron microscopy (TEM), selected area electron diffraction (SAED), and high-resolution TEM (HRTEM). Figure 1g presents a representative TEM image of the as-transformed Te nanoplates; this image suggests that the solid Sb_2Te_3 hexagonal nanoplates were transformed into the porous Te hexagonal plates, but the plate-like macroscopic morphology remained unchanged. The inset of Figure 1g displays the SAED pattern, which was recorded with the incident electron beam perpendicular to the wide surface of the plate, of one porous nanoplate. Interestingly, regular diffraction spots are observed, thus indicating the single-crystal-like structure of the porous network-structured Te disk. Through extensive investigations on individual nanoplates from the tellurium products with SAED, we found that the single-crystal-like character of the 3D porous Te plate were maintained in all of the products. The high-magnification TEM image (Figure 1h) clearly shows that the porous nanoplates are composed of solid nanothreads with a diameter of 50–100 nm. It can be clearly seen from Figure 1h that the nanothreads in the porous products are quite flexible. The clearly observed fringe spacing of 0.32 nm in the HRTEM image shown in Figure 1i corresponds to the separation of the (101) lattice plane of Te, therefore further indicating that the Sb_2Te_3 plates can be transformed into single-crystal-like porous Te nanoplates.

To clarify the chemical transformation mechanism, SEM, EDX, and ICP (inductively coupled plasma emission spectroscopy) were used to characterize the intermediates collected at different stages of the reaction. After the reaction had proceeded for 0.5 hours, the surface of hexagonal plate-like samples became very rough (Figure 2b). The associated EDX spectrum and ICP(Figure S3 in the Supporting Information) revealed that the intermediates' atomic ratio of Te to

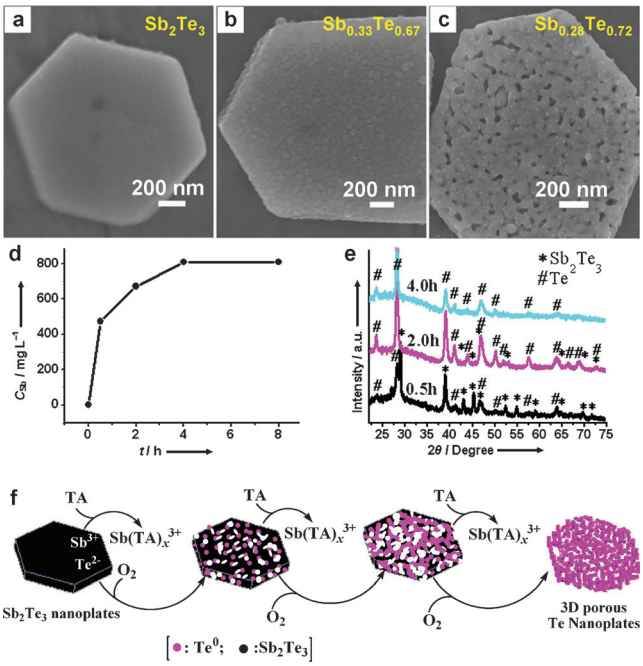

Figure 2. Typical SEM images and the associated composition of a) the starting Sb_2Te_3 nanoplate, and b) the intermediates collected at 0.5 h and c) the intermediates collected at 2 h. The compositions were determined by EDX spectra and ICP. d) Dependence of the concentration of antimony in aqueous solution on the reaction time. e) XRD pattern of the intermediates collected at different reaction times. f) Schematic illustration of the proposed chemical transformation mechanism of Sb_2Te_3 solid nanoplates into 3D porous network-structured Te plates induced by TA and oxygen.

Sb is approximately 2.0, which is higher than the initial ratio (Te/Sb = 1.5) of the starting Sb_2Te_3 materials. This indicates that the Sb composition of the samples is rapid decreasing. The decreasing ratio in the samples may be attributed to the appearance of a soluble species (recorded as $Sb(TA)_x^{3+}$) from the coordination of the Sb^{3+} ions in Sb_2Te_3 with TA, as observed for cadmium ions of CdTe in EDTA.[5a] This speculation on the dissolution of the Sb^{3+} ions in the chemical transformation is further confirmed by the increase of antimony concentration in the aqueous solution, as shown in Figure 2d. The XRD patterns of the intermediates (Figure 2e) show that the intermediates collected at 0.5 hours are composed of Sb_2Te_3 and Te, thus confirming that Te^{2-} ions in the starting materials are partially converted into Te^0. When the reaction proceeds for 2 hours, the porous structure with the higher ratio of Te to Sb (2.57) appears. A prolonged transformation reaction time led to a higher composition of

Te^0 and a more obvious porous network (Figure 2c), and finally generated 3D porous network-structured Te plates after 6 hours (Figure 1b and Figure S1 in the Supporting Information). In the corresponding XRD patterns of the intermediates, the diffraction peaks from Sb_2Te_3 firstly decreased and then disappeared after 4 hours (Figure 2e), but the Te peaks increased during chemical transformation. This finding testifies that the complete chemical conversion of Sb_2Te_3 into porous network-structured Te can be realized through the solution-phase stripping of Sb^{3+} ions from Sb_2Te_3.

To further explore the reaction mechanism, the role of TA on the chemical and structural transformation was studied. In the absence of TA, only a slight change to the surface of the hexagonal nanoplates occurred without an obvious change to the composition, as displayed in Figure S4 in the Supporting Information. This implies that TA played an important role in the chemical transformation of solid Sb_2Te_3 nanoplates into porous network-structured Te plates. We also found that the concentration of TA exerted a remarkable influence on the final morphology and composition of the products obtained through such chemical conversion. A high concentration of TA resulted in a mixture of wire-like Te and porous Te plates (Figure S5 in the Supporting Information). When citric acid is used to replace TA and other experimental conditions remain unchanged, 3D porous network-structured Te plates can also be obtained (Figure S6 in the Supporting Information), thus indicating that citric acid can promote the dissolution of antimony in Sb_2Te_3. This result suggests that the combination of organic molecules with Sb^{3+} ions to form soluble complexes may be used to treat solid binary semiconductor nanomaterials and produce novel materials that cannot be obtained otherwise. The effect of oxygen on the chemical transformation reaction was also investigated. When the chemical conversion reaction was performed under an Ar atmosphere and other experimental parameters were kept unchanged, the final products were mainly Sb_2Te_3 (Figure S7 in the Supporting Information). However, excess oxygen gave rise to the destruction of the plate-like morphology of Te and even resulted in the formation of white oxides. Additionally, it was found that the reaction temperature is an important factor to determine the morphology and composition of the products (Figure S8 in the Supporting Information).

Based on these above-mentioned results, we propose the following mechanism, involving TA and oxygen, for the chemical conversion of hexagonal Sb_2Te_3 nanoplates into 3D network-structured porous Te nanoplates (Figure 2f). Firstly, TA attacks the Sb^{3+} ions at elevated temperature, and then removes an antimony ion from Sb_2Te_3 through the formation of $Sb(TA)_x^{3+}$. Meanwhile, Te^{2-} ions on the surface are released into the solution. Then, the Te^{2-} ions are oxidized by O_2 to Te^0. The nucleation and growth of Te^0 preferentially takes place on a substrate rather than in an homogeneous solution because the required level of supersaturation on the Sb_2Te_3 substrate is lower than in solution.[9] These as-formed Te nuclei are used as the seeds for the further growth of Te. A prolonged chemical transformation time results in the continuous stripping of the Sb^{3+} ions from the surface of Sb_2Te_3 and the oxidation of Te^{2-} ions to Te^0. The oxidation of Te^{2-} ions provides the Te source for further growth of the Te plate. The continuous dissolution of antimony leads to the appearance of some channels for the release of $Sb(TA)_x^{3+}$ into solution. When the antimony source of Sb_2Te_3 is completely consumed, these channels remain, and become pores in the final products (Figure 1b and Figure 2). Finally, kinetically stable 3D nanothread-based porous Te plates with a single-crystal-like structure, form through an Ostwald ripening mechanism.[10] Under high concentration of TA, the quick depletion of the Sb^{3+} ions, the simultaneous release of Te^{2-} ions, and their subsequent rapid oxidation to Te, will make the aqueous solution immediately reach the supersaturation of Te nuclei. Therefore, the further growth of Te occurs simultaneously on the substrate and in the solution, and then gives rise to the production of a mixture of Te nanoparticles (even nanowires) and 3D Te porous network-structured plates. Note that an additional systematic study is necessary to fully explore fundamental issues of size- and shape-dependent conversion activity and its generality, for this chemical transformation strategy.

On the basis of the chemical transformation mechanism, the synthesis of heterogeneous In/Te porous networks can be achieved. When $InCl_3$ is added to the initial reaction solution, In^{3+} ions are reduced by tartaric acid (Figure S9 in the Supporting Information) or Te^{2-} ions to form In^0, and then In nucleates and grows on the as-formed Te networks because of a required lower level of supersaturation on the Te substrate than that in the solution.[9] This reaction finally generates heterogeneous In/Te porous networks, as confirmed by SEM image and EELS mapping images (Figure S10 in the Supporting Information).

The resulting 3D porous network-structured Te nanoplates can be adopted as templates to produce novel 3D porous functional nanoplates. Figure 3 gives the SEM and TEM images of 3D porous Pt plates; these images suggest the

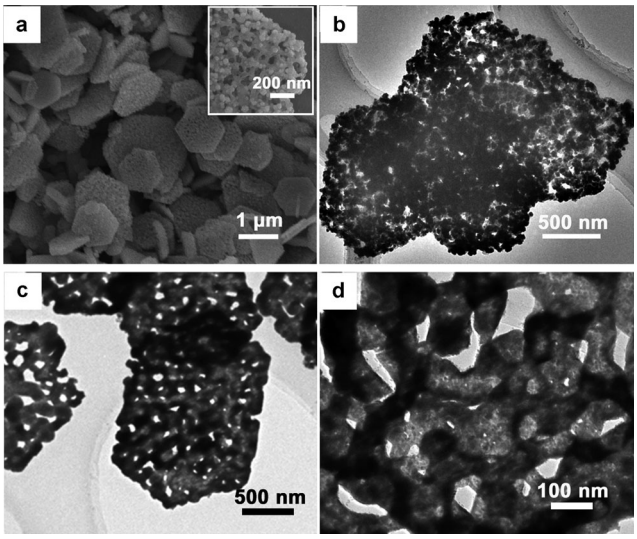

Figure 3. a) SEM image and b) TEM image of the porous nanothread-based Pt plates synthesized through the galvanic reaction of metal salt using porous network-structured Te templates. c,d) TEM images of the porous nanotube-based Pd plates synthesized through the galvanic reaction between $PdCl_2$ and porous network-structured Te templates and the subsequent removal of Te templates.

large-scale production of porous network-structured Pt plates. A high-resolution TEM image (Figure S11c in the Supporting Information) revealed that the porous Pt networks are composed of sub-5 nm highly crystalline Pt nanoparticles, which may exhibit improved catalytic properties. Additionally, porous Au plates can be successfully fabricated through the galvanic reaction between the as-prepared porous Te plates and $HAuCl_4$ (Figure S11 in the Supporting Information). Interestingly, novel porous nanotube-based Pd plates can be created by the controlled galvanic reaction between porous network-structured Te plates and $PdCl_2$, and the subsequent removal of the Te templates (Figure 3c,d and Figure S12 in the Supporting Information). These novel porous 3D nanotube-based (or solid-nanothread-based) noble-metal nanoplates should find promising applications because noble-metal nanomaterials have been considered to be one of the most important materials in electrocatalysis,[6b,11] plasmonics,[11] fuel cells,[12] sensors,[13] and heterogeneous organic catalysis.[14] In addition to the well-known good photoconductivity of Te nanowires,[15] Te nanowires have been proved to be ideal templates to create novel one-dimensional materials, involving Pt, Te-Pt, Pd, Au, Ag_2Te, PbTe and CdTe nanostructures.[2e,16] Thus, the as-prepared porous network-structured Te plate could possibly be used as a general template to produce porous nanotube-based (or solid-nanothread-based) plates of metal tellurides with potential applications in electronics.[17] Additionally, single-crystal-like porous network-structured Te plates may exhibit intriguing optoelectronic properties.[15]

In conclusion, we have developed a new route to induce a drastic structural and compositional transformation of Sb_2Te_3 nanoplates into 3D porous network-structured Te nanoplates. The reaction mechanism involves the dissolution of Sb_2Te_3 by the coordination of the Sb^{3+} ions with tartaric acid, a subsequent oxygen-assisted oxidation of the Te^{2-} ions to Te^0 and subsequent growth of the network at elevated temperatures. In the process, the addition of In^{3+} ions results in the production of porous heterogeneous In/Te nanoplates. This chemical transformation strategy from nanotemplates into derivative porous products with morphological retention can be considered as a new addition to the growing toolbox of "conversion chemistry" reactions.[2–5,7d,18] In addition, porous network-structured Te nanoplates can be used as templates to prepare high-quality porous nanothread-based noble-metal nanoplates and porous nanotube-based Pd plates. It is expected that the porous Te templates will be desirable for creating other porous functional metal and metal tellurides (e.g. CdTe, PbTe, Ag_2Te). These porous nanostructures can be of special interest for a variety of applications, including electrocatalysis, organic catalysis, sensors, separation, photoelectronics, and nanoelectronics.

Received: October 23, 2011
Published online: January 3, 2012

Keywords: chemical transformation · mesoporous materials · nanostructures · tellurium · template synthesis

[1] a) H. G. Yang, C. H. Sun, S. Z. Qiao, J. Zou, G. Liu, S. C. Smith, H. M. Cheng, G. Q. Lu, *Nature* **2008**, *453*, 638; b) J. Liu, S. Z. Qiao, S. B. Hartono, G. Q. Lu, *Angew. Chem.* **2010**, *122*, 5101; *Angew. Chem. Int. Ed.* **2010**, *49*, 4981; c) B. S. Shim, Z. Tang, M. P. Morabito, A. Agarwal, H. Hong, N. A. Kotov, *Chem. Mater.* **2007**, *19*, 5467; d) J. Zhu, B. S. Shim, M. Di Prima, N. A. Kotov, *J. Am. Chem. Soc.* **2011**, *133*, 7450; e) Z. Mao, R. Cartier, A. Hohl, M. Farinacci, A Dorhoi, T. L. Nguyen, P. Mulvaney, J. Raltston, S. H. E. Kaufmann, H. Höhwald, D. Wang, *Nano Lett.* **2011**, *11*, 2152; f) C. H. Cho, C. O. Aspetti, M. E. Turk, J. M. Kikkawa, S. W. Nam, R. Agarwal, *Nat. Mater.* **2011**, *10*, 669.

[2] a) M. Saruyama, M. Kanehara, T. Teranishi, *J. Am. Chem. Soc.* **2010**, *132*, 3280; b) R. Li, Z. Luo, F. Papadimitrakopoulos, *J. Am. Chem. Soc.* **2006**, *128*, 6280; c) F. Wang, Y. Han, C. S. Lim, Y. Lu, J. Wang, J. Xu, H. Chen, C. Zhang, M. Hong, X. Liu, *Nature* **2010**, *463*, 1061; d) F. Meng, S. A. Morin, S. Jin, *J. Am. Chem. Soc.* **2011**, *133*, 8408; e) G. D. Moon, S. Ko, Y. Xia, U. Jeong, *ACS Nano* **2010**, *4*, 2307.

[3] a) D. H. Son, S. M. Hughes, Y. Yin, A. P. Alivisatos, *Science* **2004**, *306*, 1009; b) R. D. Robinson, B. Sadtler, D. O. Demchenko, C. K. Erdonmez, L. W. Wang, A. P. Alivisatos, *Science* **2007**, *317*, 355; c) S. E. Wark, C. H. Hsia, D. H. Son, *J. Am. Chem. Soc.* **2008**, *130*, 9550; d) B. Zhang, Y. Jung, H. S. Chung, L. van Vugt, R. Agarwal, *Nano Lett.* **2010**, *10*, 149; e) Z. Tang, P. Podsiadlo, B. S. Shim, J. Lee, N. A. Kotov, *Adv. Funct. Mater.* **2008**, *18*, 3801; f) J. Yang, Y. Zhou, S. Zheng, X. Liu, X. Qiu, Z. Tang, R. Song, Y. He, C. W. Ahn, J. W. Kim, *Chem. Mater.* **2009**, *21*, 3177.

[4] a) A. Ben Moshe, G. Markovich, *Chem. Mater.* **2011**, *23*, 1239; b) M. V. Kovalenko, D. V. Talapin, M. A. Loi, F. Cordella, G. Hesser, M. I. Bodnarchuk, W. Heiss, *Angew. Chem.* **2008**, *120*, 3071; *Angew. Chem. Int. Ed.* **2008**, *47*, 3029; c) Y. D. Yin, R. M. Rioux, C. K. Erdonmez, S. Hughes, G. A. Somorjai, A. P. Alivisatos, *Science* **2004**, *304*, 711; d) A. E. Henkes, Y. Vasquez, R. E. Schaak, *J. Am. Chem. Soc.* **2007**, *129*, 1896; e) H. J. Fan, M. Knez, R. Scholz, K. Nielsch, E. Pippel, D. Hesse, M. Zacharias, U. Gosele, *Nat. Mater.* **2006**, *5*, 627.

[5] a) Z. Tang, Y. Wang, K. Sun, N. A. Kotov, *Adv. Mater.* **2005**, *17*, 358; b) Z. Tang, Y. Wang, S. Shanbhag, M. Giersig, N. A. Kotov, *J. Am. Chem. Soc.* **2006**, *128*, 6730.

[6] a) J. Liu, S. Z. Qiao, Q. H. Hu, G. Q. Lu, *Small* **2011**, *7*, 425; b) C. X. Xu, Y. Zhang, L. Q. Wang, L. Q. Xu, X. F. Bian, H. Y. Ma, Y. Ding, *Chem. Mater.* **2009**, *21*, 3110; c) Z. Peng, H. Yang, *J. Am. Chem. Soc.* **2009**, *131*, 7542; d) C. H. Cui, H. H. Li, S. H. Yu, *Chem. Sci.* **2011**, *2*, 1611; e) Y. Li, W. Cai, B. Cao, G. Duan, F. Sun, C. Li, L. Jia, *Nanotechnology* **2006**, *17*, 238; f) Y. Xu, L. Zhang, C. Wu, F. Qi, Y. Xie, *Chem. Eur. J.* **2011**, *17*, 384.

[7] a) H. E. Elsayed-Ali, T. Juhasz, G. O. Smith, W. E. Bron, *Phys. Rev. B* **1991**, *43*, 4488; b) H. Idriss, K. S. Kim, M. A. Barteau, *J. Catal.* **1993**, *139*, 119; c) A. Kudo, Y. Miseki, *Chem. Soc. Rev.* **2009**, *38*, 253; d) Y. Yu, J. Zhang, X. Wu, W. Zhao, B. Zhang, *Angew. Chem. Int. Ed.* **2012**, DOI: 10.1002/anie.201105786.

[8] W. Shi, L. Zhou, S. Song, J. Yang, H. Zhang, *Adv. Mater.* **2008**, *20*, 1892.

[9] a) D. S. Boyle, K. Govender, P. O'Brien, *Chem. Commun.* **2002**, 80; b) B. Zhang, X. Ye, C. Wang, Y. Xie, *J. Mater. Chem.* **2007**, *17*, 2706.

[10] a) B. Mayers, Y. N. Xia, *Adv. Mater.* **2002**, *14*, 279; b) B. Mayers, Y. N. Xia, *J. Mater. Chem.* **2002**, *12*, 1875.

[11] a) Z. Y. Zhou, X. Kang, Y. Song, S. Chen, *Chem. Commun.* **2011**, *47*, 6075; b) X. Huang, S. Tang, X. Mu, Y. Dai, G. Chen, Z. Zhou, F. Ruan, Z. Yang, N. Zheng, *Nat. Nanotechnol.* **2011**, *6*, 32; c) M. Jin, H. Zhang, Z. Xie, Y. Xia, *Angew. Chem.* **2011**, *123*, 7996; *Angew. Chem. Int. Ed.* **2011**, *50*, 7850; d) M. Jin, H. Zhang, Z. Xie, Y. Xia, *Angew. Chem.* **2011**, *123*, 7996; *Angew. Chem. Int. Ed.* **2011**, *50*, 7850.

[12] a) X. Ji, K. T. Lee, R. Holden, L. Zhang, J. Zhang, G. A. Botton, M. Couillard, L. F. Nazar, *Nat. Chem.* **2010**, *2*, 286; b) Y. Xu, S. Hou, Y. Liu, Y. Zhang, H. Wang, B. Zhang, *Chem. Commun.* **2012**, DOI: 10.1039/C2CC16798K.
[13] W. Chen, N. B. Zuckerman, J. P. Konopelski, S. Chen, *Anal. Chem.* **2010**, *82*, 461.
[14] a) M. Crespo-Quesada, A. Yarulin, M. Jin, Y. Xia, L. Kiwi-Minsker, *J. Am. Chem. Soc.* **2011**, *133*, 12787; b) A. Wittstock, V. Zielasek, J. Biener, C. M. Friend, M. Bäumer, *Science* **2010**, *327*, 319.
[15] a) J. W. Liu, J. H. Zhu, C. L. Zhang, H. W. Liang, S. H. Yu, *J. Am. Chem. Soc.* **2010**, *132*, 8945; b) Y. Wang, Z. Tang, P. Podsiadlo, Y. Elkasabi, J. Lahann, N. A. Kotov, *Adv. Mater.* **2006**, *18*, 518.
[16] a) J. Yuan, H. Schmalz, Y. Xu, N. Miyajima, M. Drechsler, M. W. Möller, F. Schacher, A. H. E. Müller, *Adv. Mater.* **2008**, *20*, 947; b) B. Zhang, W. Hou, X. Ye, S. Fu, Y. Xie, *Adv. Funct. Mater.* **2007**, *17*, 486; c) H. W. Liang, S. Liu, J. Y. Gong, S. B. Wang, L. Wang, S. H. Yu, *Adv. Mater.* **2009**, *21*, 1850; d) H. W. Liang, S. Liu, Q. S. Wu, S. H. Yu, *Inorg. Chem.* **2009**, *48*, 4927; e) B. Mayers, X. C. Jiang, D. Sunderland, B. Cattle, Y. N. Xia, *J. Am. Chem. Soc.* **2003**, *125*, 13364; f) X. C. Jiang, B. Mayers, T. Herricks, Y. Xia, *Adv. Mater.* **2003**, *15*, 1740.
[17] a) S. L. Teich-McGoldrick, M. Bellanger, M. Caussanel, L. Tsetseris, S. T. Pantelides, S. C. Glotzer, R. D. Schrimpf, *Nano Lett.* **2009**, *9*, 3683; b) J. He, J. R. Sootsman, S. N. Girard, J. C. Zheng, J. G. Wen, Y. M. Zhu, M. G. Kanatzidis, V. P. Dravid, *J. Am. Chem. Soc.* **2010**, *132*, 8669.
[18] a) I. T. Sines, R. E. Schaak, *J. Am. Chem. Soc.* **2011**, *133*, 1294; b) E. F. Rodriguez, P. Zavalij, P. Y. Hsieh, M. A. Green, *J. Am. Chem. Soc.* **2010**, *132*, 10006.

